David Florián-Algarín*, Alexandra Padilla, Neshma N. López and Oscar Marcelo Suárez

Fabrication of aluminum wires treated with nanocomposite pellets

Abstract: This study focuses on the fabrication of aluminum treated with nanocomposites made of aluminum and NbB_2 and ZrB_2 nanoparticles. These nanoparticles were obtained by fragmentation in a ball mill and then mechanically alloyed with pure aluminum powder to form Al/NbB_2 and Al/ZrB_2 nanocomposite pellets, which were then sintered at 260°C for half an hour to improve the metal/borides interface. The sintered nanocomposites were incorporated into molten pure aluminum to produce 1-mm-diameter wires after cold forming. The wire specimens were mechanically characterized and their electrical resistivity was measured. Our results demonstrated the feasibility of improving the mechanical properties of aluminum wires with the addition of nanocomposites without significantly affecting their electrical conductivity.

Keywords: aluminum; nanocomposite; wires.

***Corresponding author: David Florián-Algarín,** Department of Mechanical Engineering, University of Puerto Rico-Mayaguez, PO Box 9000, Mayaguez PR 00681-9000, e-mail: david.florian@upr.edu
Alexandra Padilla: Department of Mechanical Engineering, University of Puerto Rico-Mayaguez, PO Box 9000, Mayaguez PR 00681-9000
Neshma N. López: Department of Chemical Engineering, University of Puerto Rico-Mayaguez, PO Box 9000, Mayaguez PR 00681-9000
Oscar Marcelo Suárez: Department of General Engineering, University of Puerto Rico-Mayaguez, PO Box 9000, Mayaguez PR 00681-9000

1 Introduction

A main challenge for the aerospace industry has been to create low fabrication cost materials that are more energy efficient [1]. For this reason, advanced commercial aircraft used mostly optical fibers and aluminum wires rather than more dense copper [2]. Aluminum possesses high electrical conductivity compared with other metals and ranks fourth among metals with the lowest resistivity. As aluminum's high ductility and low melting point may create problems, such as extensive and undesired plastic deformations, the present project focuses on the reinforcement of aluminum wires by adding zirconium diboride (ZrB_2) or niobium diboride (NbB_2) nanoparticles embedded in an aluminum matrix to increase the stiffness and strength of the metal and to study the resulting electrical resistivity of the wires.

ZrB_2 and NbB_2 possess an appealing combination of high melting point, high electrical and thermal conductivity, chemical inertness in contact with many molten metals or non-basic slags, and superb thermal shock resistance [3, 4]. Also, the diborides bear good mechanical properties and resistance to corrosion [5].

Moreover, aluminum wires with the desired cross-sectional area can be readily obtained by cold drawing. High-quality wires can then be drawn by adjusting recrystallization temperatures while taking into account strain hardening and yielding of aluminum. Earlier work showed that such cold deformation should not significantly affect the resulting electrical conductivity of the aluminum wire [6].

2 Materials and methods

In a prior research, a vario-planetary high-energy ball mill (Pulverisette 4, manufactured by Fritsch GmbH, Idar-Oberstein, Germany) was demonstrated to be practicable in reducing diboride particle sizes by fragmentation [7]. The same equipment allowed fracturing as-received NbB_2 (Aremco Products, Valley Cottage, NY, USA) and ZrB_2 (AlfaAesar, Ward Haverhill, MA, USA) particles to obtain nanostructured particles of the diborides. The high-energy ball mill operated at 1600 rpm with tungsten carbide grinding balls of 11.2-mm diameter. The diboride powders were then milled with pure aluminum powder (Acros Organics, Morris Plains, NJ, USA) for 1 h to form diboride/Al nanocomposite pellets with an average size of 0.3 mm. These were then sintered at 260°C for a half hour in a reduced vacuum atmosphere (roughly 4 kPa) in order to increase the homogenization of the pellets and enhance the aluminum/diboride interface. The incorporation of aluminum into the pellet to form the nanocomposites allowed for better wetting by molten aluminum upon inoculation.

Pure aluminum (99.5%) was then melted at 760°C in a graphite crucible, inoculated with the sintered pellets, and mechanically stirred to improve the particle distribution. The treated melt was then poured into a cylindrical mold to produce 5-mm-diameter ingots, which we cold-rolled to obtain wires of 1.4-mm diameter with a cross-area reduction of 92%. Full annealing at 400°C for 5 h permitted the cold rolling to continue so as to reduce the wire diameter to 1 mm with a final cross-area reduction of 96%.

All samples were characterized by X-ray diffraction (XRD) using a Siemens® (Princeton, NJ, USA) D500 diffractometer with Cu Kα radiation (λ=0.154178 nm). This procedure helped to (a) estimate both the nanoparticle size of NbB_2 and ZrB_2 using Scherrer's equation [8] and (b) to analyze the XRD patterns of the composite pellets so as to determine whether unintended phases were formed upon milling. The microstructures of the specimens, i.e., as-received powder, pellets, and wires (at different stages of the manufacturing process), were observed using a Nikon® (Melville, NY, USA) Model Epiphot 200 optical microscope and scanning electron microscope (SEM). Standard tensile tests at room temperature (25°C) were conducted in a low-force Instron® model 5944 universal testing machine (Norwood, MA, USA).

A four-point probe technique was used to measure the wires' electrical resistivity using a convenient setup developed in a prior investigation [9]. This method measures the voltage between two probing points while the different levels of current are applied via two electrodes. Then, by measuring the sample geometry, one can compute the wire resistivity. The setup can also be immersed into ice water and boiling water (100°C) to study how temperature affects the resistivity of the wires. The wires' electrical conductivity measurement was carried out at temperatures ranging from 0°C to 100°C. Finally, electrical conductivity (inverse of the measured resistivity ρ) is expressed in terms of percent of the International Annealed Copper Standard (IACS) [10].

3 Results

3.1 Diboride nanoparticles

To determine the most efficient milling procedure needed to produce the nanoparticles, different times were tested, ranging from 5 to 25 h for the NbB_2, whereas ZrB_2 powder was obtained at 5 and 10 h. As mentioned, Scherrer's equation allowed estimating of the average size of the ball-milled diboride samples based on the width of the largest peak. Subsequent millings at different times helped determine that after 10 h the particle size remained almost constant, i.e., regardless of the milling time, as shown in Figure 1.

The SEM images in Figure 1 show NbB_2 particles before the ball milling process and after 10 milling hours. The reduction in particle size of the diboride is apparent. The NbB_2 particles obtained, which were milled for 10 h, had an approximate size of 17 nm, which was deemed appropriate to proceed with the planned experiments.

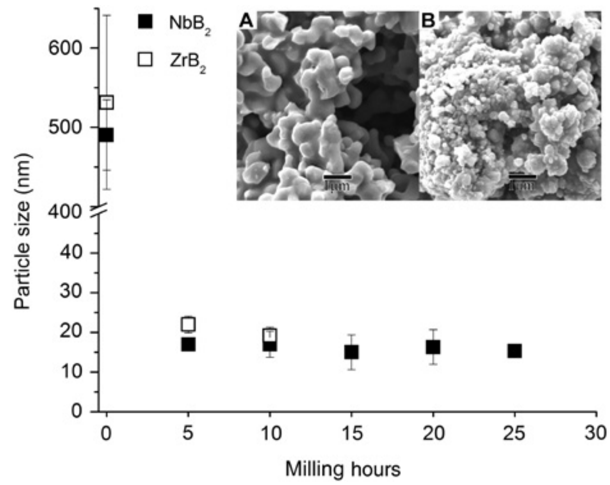

Figure 1 Average computed NbB_2 and ZrB_2 particle size as a function of milling time. In the inset, one can observe secondary electron images of the NbB_2 particles: (A) as-received NbB_2 (without ball milling) and (B) clusters of NbB_2 particles after 10 milling hours.

3.2 Nanocomposite pellets

The nanosized diboride particles and pure 99.5% aluminum powder (average size of 44 μm) were mixed at 1000 rpm for 1 h in the same ball milling unit to form the Al/diboride pellets. As mentioned, all nanocomposite pellets were then sintered at 260°C in a reduced vacuum atmosphere. Figure 2 shows the XRD patterns obtained from Al/NbB_2 and Al/ZrB_2 nanocomposites. It is apparent that no additional unintended phase was accidentally produced during the pellet fabrication.

Figure 3 shows representative microstructures of the sintered pellets. The images allowed corroborating that diboride nanoparticles were well embedded in the Al matrix after milling to form the nanocomposites.

3.3 Optical micrographs of wires

Figure 4A through C presents the microstructure of the aluminum wires at different stages of the manufacturing process, as observed in an optical microscope. Figure 4A shows the grain structure of as-cast ingot treated with 1 wt% of NbB_2, i.e., before cold working. In Figure 4B, we can observe how the grains in the Al-2 wt% NbB_2 ingot are

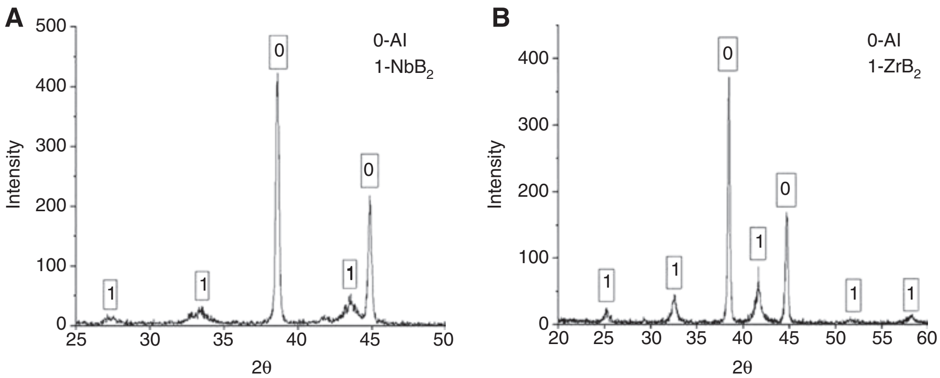

Figure 2 XRD pattern of pellets. (A) Al/NbB_2 composite pellet after sintering, (B) Al/ZrB_2 composite pellet after sintering.

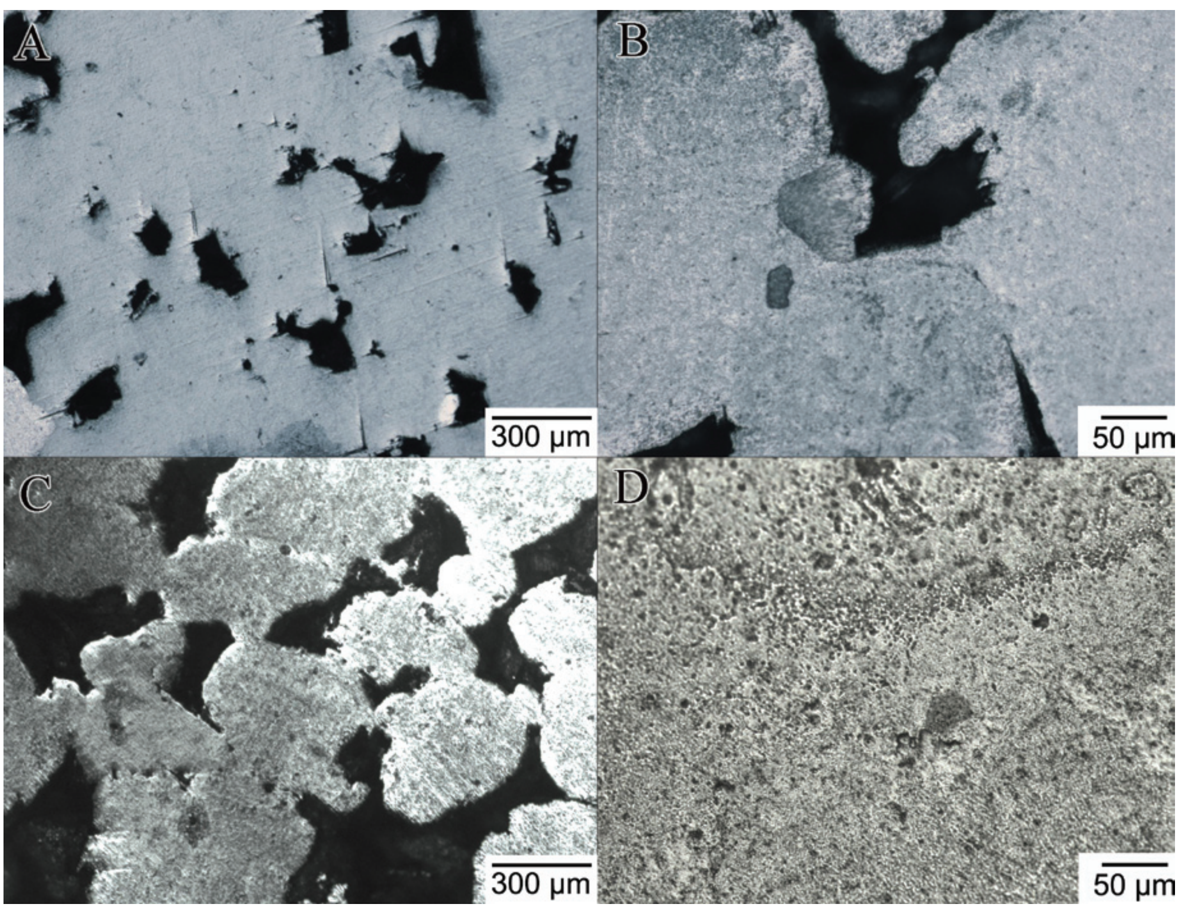

Figure 3 Optical micrographs of the nanocomposite pellets: (A) Al/NbB_2 pellet at low magnification, (B) Al/NbB_2 pellet at higher magnification, (C) Al/ZrB_2 pellet at low magnification, and (D) Al/ZrB_2 pellet at higher magnification.

deformed with 92% cross-area reduction. In Figure 4C, the grain structure of the cold-formed specimen changes after full annealing is apparent. Full annealing at 400°C for 5 h permitted grain recrystallization, as seen in Figure 4C. In Figure 4D, one can observe the grains of the final wire produced.

3.4 Electrical conductivity

In the case of wires treated with NbB_2, the conductivity decreased from 62.7% to 57.3% IACS at 20°C for NbB_2 concentrations from 0% to 3%, as observable in Figure 5A. Figure 5B appears to demonstrate that for ZrB_2, there is

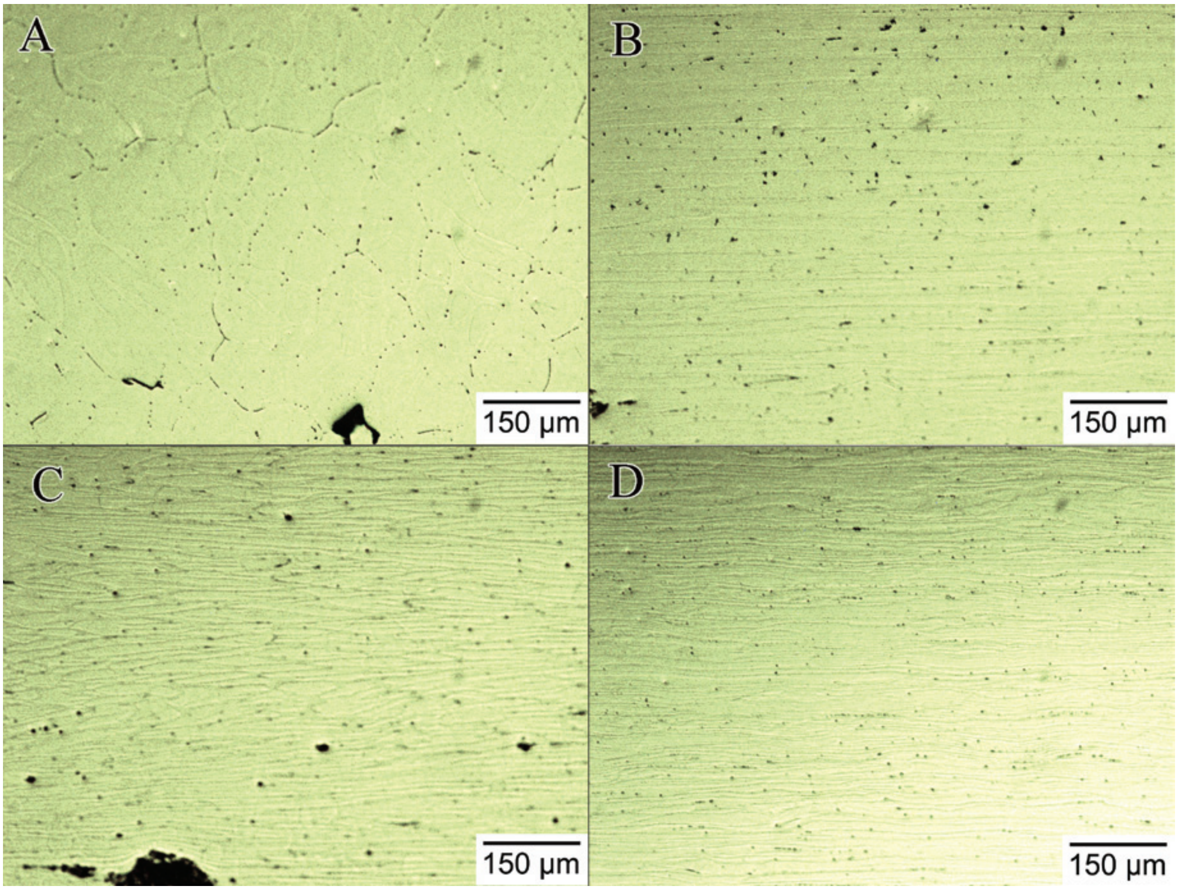

Figure 4 Microstructures of the wires at different stages of the manufacturing process. (A) Aluminum ingot treated with 1 wt% of NbB_2 particles contained in the nanocomposite pellet, (B) aluminum wire containing 1 wt% of NbB_2 after cold rolling, (C) aluminum with 1% NbB_2 after annealing, (D) final sample of Al-1% NbB_2 wire of 1-mm diameter.

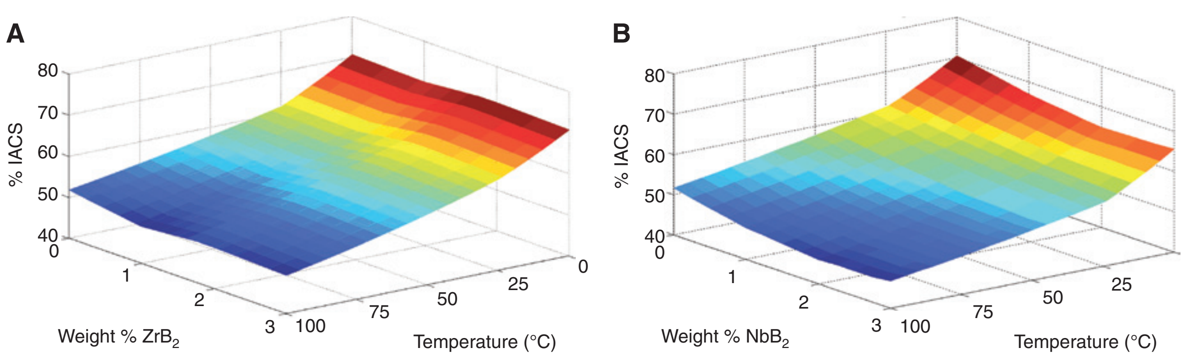

Figure 5 Effect of amounts of diborides added and temperature on the electrical conductivity of aluminum wires (measured as percent of IACS): (A) effect of the ZrB_2/Al nanocomposite, (B) effect of the ZrB_2/Al nanocomposite.

no significant change in the conductivity as the amount of nanoparticles increases. In both cases (NbB_2 and ZrB_2), naturally, the resistivity increases almost linearly with temperature.

3.5 Tension tests

As we can see, for both of the diborides studied, the minimum tensile strength increases as the amount of diboride nanoparticles added increases. The achieved tensile strengths of the aluminum wires are much higher than the strength normally reported for pure aluminum, i.e., 70 MPa [11].

4 Discussion

As observed in Figure 6, the electrical conductivity of the wires treated with ZrB_2/Al nanocomposite remains constant with a value over 63% IACS at 20°C (close to pure aluminum) for all the additions. We attributed this result to the low resistivity of ZrB_2, reported as 4.6 μΩ cm [12].

However, the electrical conductivity of the wires treated with NbB_2 nanoparticles reduced slightly. To verify the statistical significance of the addition effects of both ZrB_2 and NbB_2 on the electrical conductivity of the wires, we carried out a multiple linear regression study. Eqs. (1) and (2) are the resulting descriptive models of the electrical conductivity with respect to the amount of diborides added and the temperature. The nomenclature used in the equations is as follows: %IACS=percent of International Annealed Copper Standard; T=temperature (°C); MTS=minimum tensile strength (MPa); $\%NbB_2$=wt% of NbB_2 and $\%ZrB_2$=wt% of ZrB_2. The values of the coefficients of multiple determinations R^2 for both models, i.e., NbB_2 and ZrB_2 nanocomposite additions, are very high: 87.99% and 93.93%, respectively. This indicates that both linear models [Eqs. (1) and (2)] explain all the variability of the response data. The resulting analysis of variance (ANOVA) table (Table 1) further displays the fitting parameters and p values for both models, i.e., wires containing $\%NbB_2$ and $\%ZrB_2$.

$$\%IACS=67.3481\text{-}1.00294(\%NbB_2)\text{-}0.178683T \quad (1)$$

$$\%IACS=68.5473+0.0432053(\%ZrB_2)\text{-}0.191377T \quad (2)$$

For the model in Eq. (1), i.e., wires treated with NbB_2, the p value is just above 0.05, which indicates that increasing the addition of NbB_2/Al nanocomposite pellets barely affects the wires' electrical conductivity. For Eq. (2), the p value calculated is significantly higher than 0.05, which corroborates that the addition of ZrB_2/Al nanocomposite pellets has no detectable effect on the wires' electrical conductivity.

In Figure 6, one can observe that the measured MTS of the wires increased as a function of the amount of both NbB_2 and ZrB_2 added in the nanocomposite pellets. A linear regression analysis was implemented to model the effect of the additions of NbB_2 and ZrB_2 nanoparticles. Eqs. (3) and (4) present the computed linear models of the wires' tensile strengths as a function of the amount of NbB_2 and ZrB_2 added, respectively. Once again, the calculated coefficients of multiple determinations R^2 are very high: 99.9% for Eq. (3) (NbB_2 added) and 96.0% for Eq. (4) (ZrB_2 added). Table 2 presents the ANOVA of the linear regression models in Eqs. (3) and (4), respectively.

$$MTS\,(MPa)=93.6+7.04(\%NbB_2) \quad (3)$$

$$MTS\,(MPa)=93.4+8.11(\%ZrB_2) \quad (4)$$

For both models, the standard error of the fitted coefficients in Eqs. (3) and (4) are small. Particularly, the computed p values are near zero, which indicates that the diboride amounts are very effective in strengthening the wires, with ZrB_2 bearing a larger effect. Further analysis of the fracture would be needed to assess the beneficial effect of this diboride in the strength of the aluminum wire in order to understand the strengthening mechanism associated with these results. In summary, comparing the treated ZrB_2 and NbB_2 samples shows that both tensile strength and conductivity obtained for ZrB_2-treated wires were higher than for NbB_2-treated ones. One additional advantage is that as-received ZrB_2 particles are nowadays 30% cheaper than NbB_2 particles, which make the ZrB_2 particles an appealing candidate to be used in future applications in the aluminum reinforcement.

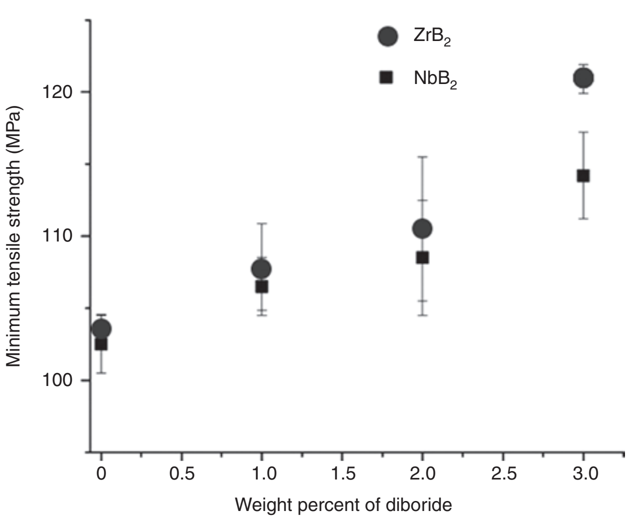

Figure 6 Measured MTS of aluminum wire samples as a function of the amount of diboride added.

Table 1 ANOVA of the models in Eqs. (1) and (2).

Parameter	%NbB_2			%ZrB_2		
	Value	Standard error of the coefficient	p-Value	Value	Standard error of the coefficient	p-Value
Constant	67.3481	1.20027	0.0000	68.5473	0.956345	0.0000
Temperature	-0.1787	0.01456	0.0000	-0.1914	0.010903	0.0000
% Diborides	-1.0029	0.55510	0.085	0.0432	0.424033	0.920

Table 2 ANOVA of the models in Eqs. (3) and (4) to predict the tensile strength of the wires.

Parameter	%NbB_2			%ZrB_2		
	Value	Standard error of the coefficient	p-Value	Value	Standard error of the coefficient	p-Value
Constant	93.60	0.3090	0.0000	96.40	1.6500	0.0000
% Diborides	7.04	0.1650	0.0010	8.11	0.8230	0.0010

5 Conclusions

The experimental results allowed stating several conclusions:

1. NbB_2 and ZrB_2 nanoparticles were successfully produced and added into molten Al in the form of diboride/aluminum nanocomposite pellets to fabricate Al wires.
2. Increasing levels of ZrB_2 have no effect on the aluminum wire electrical conductivity. Although NbB_2 nanoparticles slightly decreased the electrical conductivity of those wires, this effect is very small. Both results were also corroborated via statistical analysis.
3. The maximum tensile strength (MTS) of the wires increased as a function of the amount of both NbB_2 and ZrB_2 added, with the zirconium diboride being more effective in strengthening the wires.

Acknowledgments: The authors would like to thank the Materials Research Laboratory technician, Boris Rentería, and the students Raúl Marrero and Grace Rodríguez for their assistance in completing this project. This material is based upon work supported by the National Science Foundation under Grant HRD 0833112 (CREST program). The tensile testing machine used was acquired through a grant provided by the Solid Waste Management Authority of Puerto Rico.

Received August 16, 2013; accepted March 5, 2014; previously published online April 11, 2014

References

[1] Noor AK, Venneri SL, Paul DB, Hopkins MA. *Comput. Struct.* 2000, 74, 507–519.
[2] Rodriguez A. "A brand-new wiring system for the dreamliner," *SAFRAN 2007*, November, 2007, pp. 28–31.
[3] Yeh CL, Li RF. *Chem. Eng. J.* 2009, 147, 405–411.
[4] Liu Q, Han W, Zhang X, Wang S, Han J. *Mater. Lett.* 2009, 63, 1323–1325.
[5] Weng L, Han W, Li X, Hong C. *Int. J. Refract. Met. Hard Mater.* 2010, 28, 459–465.
[6] Çetinarslan CS. *Mater. Des.* 2009, 30, 671–673.
[7] Suárez OM, Vázquez J, Reyes-Russi L. *Sci. Eng. Compos. Mater.* 2009, 16, 267–276.
[8] Cullity BD, Stock SR. *Elements of X-Ray Diffraction*, 3rd ed., Prentice Hall: New Jersey, 2001, pp. 167–184.
[9] Suárez OM, Stone DS, Kailhofer CJ. *J. Mater. Educ.* 1999, 20, 341–356.
[10] National Bureau of Standards. *Copper Wire Tables*, 3rd ed., Washington Government Printing Office: Washington, DC, USA, 1914, Vol. 31.
[11] Totten GE, MacKenzie DS. In *Handbook of Aluminum*, vol. 1, CRC Press: New York, 2003, p. 67.
[12] Inoshita HK, Tani SO, Amiyama SK, Mano HA, Kasaki IA, Uda JS, Atsunami HM. *Jpn. J. Appl. Phys.* 2001, 40, 1280–1282.